



Surface acoustic waves in dynamic magnonic crystals for microwave signals processing

R.G. Kryshtal*, A.V. Medved

Fryazino Branch of Kotel'nikov Institute of Radioengineering and Electronics of Russian Academy of Sciences, Vvedensky sq., 1, Fryazino, Moscow Region 141190 Russia

ARTICLE INFO

Keywords:

Surface acoustic wave
Surface magnetostatic wave
Dynamic magnonic crystal
Yttrium iron garnet
Microwave signal processing
Nonreciprocal notch filter

ABSTRACT

Surface acoustic waves (SAW) in dynamic magnonic crystals (DMC) are considered for their use to create tunable spin-wave gadgets for processing of microwave signals. To understand the principles of operation of the proposed gadgets, the necessary basic properties of DMC created by a SAW in the structure of “yttrium iron garnet film on a substrate of gallium gadolinium garnet” are given. The prototype of the unique nonreciprocal notch filter working in the range of 3600–4100 MHz at the biasing magnetic field of 640 Oe is fabricated and its main characteristics such as dependences of the frequency and the depth of rejection pits on the frequency and power of the controlling SAW are measured. At the frequency of SAW of 41 MHz and power of 30 mW, the depth of the rejection pit reached 23 dB, the tunable shift of the notch frequency equaled to 7 MHz for a frequency change of SAW by 1 MHz. DMC with SAW may also be used for frequency shifting and modulation of microwave signals. Two configurations of prototypes of frequency shifting devices have been suggested, fabricated and their workability was shown experimentally.

1. Introduction

Surface acoustic wave (SAW) propagating in solids and layered structures containing piezoelectric layers, and magnetostatic spin waves (MSW) propagating in structures with layers of magnetic materials are widely used for information processing over the last decades. SAW devices for signal processing in the frequency range of 0.01–3 GHz and MSW devices in the frequency range of 1–20 GHz, such as delay lines, transverse and bandpass filters, generators, phase shifters, etc., are proposed and experimentally implemented. SAW devices have excellent properties for practical use: (1) the ability to create devices with independently specified frequency and phase characteristics, (2) a relatively large dynamic range and (3) relatively high thermal stability (see, for example, [1–4]).

The main advantages of MSW devices over the SAW devices are (1) essentially higher center frequencies and (2) the tunability of parameters by changing the external magnetic field. If many of SAW devices are now commercially available, except, say, for a number of sensor devices, the development of which continues also now, for the successful application of MSW devices requires additional research and development. In particular, it is desirable to eliminate the previously well-known drawbacks of spin-wave devices that prevent their widespread application: (1) insufficient temperature stability of the

parameters and (2) a relatively small dynamic range. (see for example [5,6]).

New applications of spin-wave devices in high-speed logic, where a small dynamic range, may not hinder their application, are under investigations [7–10]. Without a doubt, modern studies in magnonic will lead to the creation of new functional devices with unique characteristics.

In the present paper, we discuss the possibilities of the application of properties of spin waves in magnonic crystals created by the SAW in magnetic media for microwave signals processing. Some experimental results on testing several simple prototypes of devices such as tunable nonreciprocal notch filters, frequency shifters, and modulators are presented to illustrate their operability.

2. The concept of the dynamic magnonic crystals

The concept of the so-called magnonic crystals has given a new impetus to the development of devices that use MSW for processing information (for example [11,12]). Magnonic crystals (MC), as they were first named in [13,14], is a magnetic medium with periodic inhomogeneities, for propagating spin waves in which there are forbidden frequency gaps, defined by the period of these inhomogeneities. To date, various configurations of MC have been proposed and

* Corresponding author.

E-mail address: kryshtal-raisa@rambler.ru (R.G. Kryshtal).

experimentally tested, a number of devices using MC for information processing have been invented and their efficiency was investigated [12,15–17]. All this applies mostly to so-called static MC, magnetic periodic inhomogeneities in which are created in space and are constant in time, there is only a small number of publications devoted to the dynamic MC [18,19], in which magnetic inhomogeneities are not only in space but in time also. Dynamic MCs created by a SAW in yttrium iron garnet films at propagating surface magnetostatic waves (SMSW) were described in [20–23]. Magnetic inhomogeneities in magnetic media are created by SAW due to the effect of magnetostriiction. The basic physical phenomenon explaining the main features of such dynamic MC is “nonelastic scattering of SMSW on SAW”. This phenomenon was investigated in the eightieth years of last century [24–27]. SMSWs propagating in a magnetic material in which a SAW also propagates can be effectively scattered by this SAW when the following conditions of nonelastic scattering are met, (waves propagate collinearly):

$$\omega_r = \omega_l \pm \Omega, \quad |k_r| + |k_l| = |Q|, \quad (1)$$

where $\omega_l = 2\pi f_l$, k_l , $\omega_r = 2\pi f_r$, k_r are circular frequencies and wave numbers of incident and reflected SMSWs, $\Omega = 2\pi F$ and Q – the circular frequency and the wave number of SAW, respectively. f_l , f_r and F are linear frequencies of incident, reflected SMSWs and SAW, respectively. The sign “+” in (1) corresponds to the case of the counter-propagating of SMSW and SAW, the sign “-” corresponds to the co-propagation case. Schematic diagram illustrating Eq. (1) is shown in Fig. 1. SMSW propagating in such a media at certain frequencies, determined by the phase matching conditions of interacting waves (1), will be effectively scattered. The forbidden frequency gap arises for SMSW near the phase matching frequencies. Thus, SAW and SMSW in magnetics possess all the attributes of a magnonic crystal, to that attention was drawn in [20]. We will use the abbreviation SAW-MC to designate such magnonic crystals in this paper.

In [20–23] the main characteristics of the SAW-MCs were investigated. In [20] basic experimental results on studying of propagation SMSW in SAW-MC were described. The amplitude-frequency responses (AFR) of transmitted SMSW at different parameters of SAW had been presented. In [22] experimental results on the investigation of the influence of magnetic cubic crystallographic anisotropy onto parameters SAW-MC in YIG films were presented. The main feature of such an influence is the appearance of additional magnonic band gaps together with the normal magnonic band gap existing without anisotropy. The dependencies of the additional magnonic gaps frequencies and their depth were measured as functions of SAW frequency and power. In [21] experimental results on the nonreciprocity for SMSW in SAW-MC in YIG films on the substrate made of gadolinium gallium garnet (GGG) were presented. It was shown in [21] that the nonreciprocal properties for SMSW in SAW-MC exist in structures even with the symmetrical dispersion characteristic of SMSWs propagating in forward and backward directions.

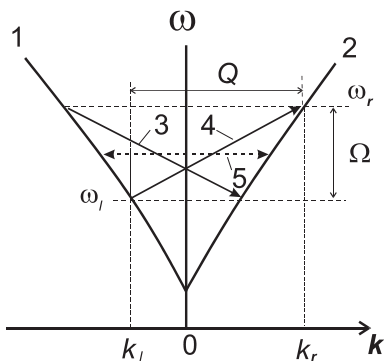


Fig. 1. Diagram ω - k explaining the interaction of waves in SAW – MC.

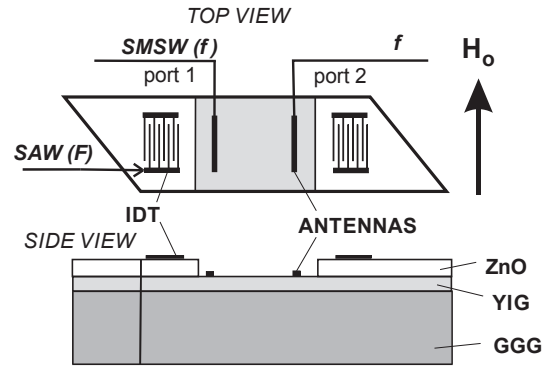


Fig. 2. The Configuration of the sample (top view and side view) for experimental investigation of microwave applications of devices based on SAW-MC.

3. Nonreciprocal tunable notch filter

Fig. 2 shows the configuration of the samples most convenient for the experimental study of SAW-MCs based on structures consisting of YIG films on GGG substrates. YIG films were grown by the method of a liquid phase epitaxy on 500- μ m-thick GGG substrate of (1 1 1) crystallographic plane. This is so-called monolithic configuration SAW-MC that has been described previously in [20]. For the excitation and detection of the SAW, thin piezoelectric films ZnO with interdigital transducers (IDT) were deposited at the edges of structures as shown in Fig. 2. The central frequency of the IDT was 41 MHz, the insertion loss of the SAW-channel in the 50-Ohm measuring circuit with matching was ~ 19 dB. SMSWs in such MCs are excited and detected by means of aluminum strips-antennas of 20- μ m- width and 0.7- μ m-thick deposited onto the surface of YIG film.

This configuration we used in our present work for demonstrating the possibilities of controllable notch filter based on SAW-MC. To reduce spurious reflections of waves from the edges, the edges of the samples have been cut off at an angle of 45 degrees as it usually does in SAW and spin-wave devices [7]. The samples were placed in the uniform magnetic field of 640 Oe directed in parallel to the antennas. Ports 1 and 2 (see Fig. 2) were used for the measurements of the amplitude-frequency response (AFR) of the S-parameters S_{12} and S_{21} in the frequency range from 3500 MHz to 4200 MHz, in which the SMSW with reasonable insertion loss (IL) existed in our experimental layout. The intensity of microwave signals applied to the ports did not exceed the value above which the nonlinear effects occurred, usually less than -3 dBm, [23].

In MCs, there are forbidden frequency zones (gaps) in which the SMSWs cannot propagate and are reflected effectively. Thus, an MC may serve as a notch filter. The bandstop frequencies in a static MC are determined by the period of the periodic magnetic inhomogeneities and cannot be changed electronically. In SAW-MCs, as shown in [20,22], the frequency of forbidden zones and their depth (center frequency and the depth of magnonic band gaps) can be changed by changing the frequency and intensity of the SAW. Thus, the SAW-MC is, in fact, electronically tunable notch filter.

Fig. 1 clarifies the functioning of notch filters based on SAW-MC graphically illustrating conditions imposed on the wave vectors and frequencies of the interacting waves (see Eq. (1)). Curves 1 and 2 in this diagram represent the branches of the dispersion curves of the SMSWs propagating in opposite directions. The arrow 3 in this picture represents the interaction between the incident and reflected SMSWs, when microwave signals are supplied to the port 1 and passed microwave signals are picked up from the port 2 (parameter S_{12} is measured). The arrow 4 represents the interaction of SMSWs when an incident wave is excited at the port 2 and a past wave is received by the port 1 (parameter S_{21} is measured). The SAW is excited by the left-hand IDT and propagates in the same direction as incident SMSW. The dotted line

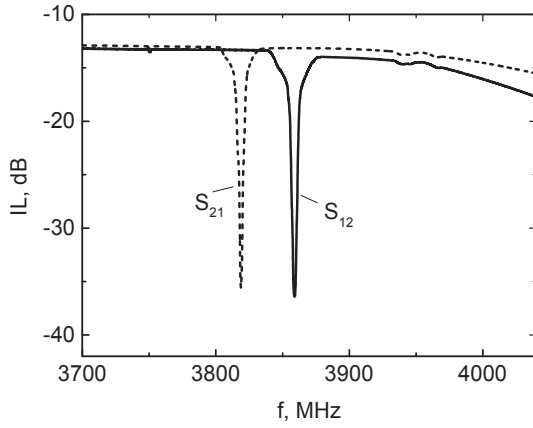


Fig. 3. Insertion loss (IL) as a function of frequency, f , (Amplitude-frequency response) of SMSW channel. SAW frequency 41 MHz. power 30 mW. IDT: 14 pairs of electrodes with 80- μ m-period. YIG film: thickness 8.6 μ m, $2\Delta H = 0.7$ Oe, distance between antennas 10 mm. Apertures of IDTs and antennas equal 5 mm. $H_0 = 640$ Oe. $T_0 = 20^\circ\text{C}$.

5 corresponding to the interaction of waves in the static MS is given here for the comparison, if the periodic magnetic inhomogeneity with the inverse lattice vector equal to the wave number of SAW would be created technologically without exciting of SAW. In this case, the incident and reflected waves would not be shifted in frequency relative to each other, and there is no nonreciprocal properties in devices based on such a structure.

The measured frequency responses $IL(f)$ of the layout, is presented in Fig. 3 as for parameter S_{12} and for S_{21} (IL is the abbreviation of the “Insertion Losses”). One can see that the frequency of the rejection changes when changing the direction of propagation of SMSW to the opposite, i.e. this notch filter has the properties of the non-reciprocity. The basic parameters of the structure used in this layout are given in the figure caption. The results are presented for both parameter S_{12} and parameter S_{21} that is, for the cases of mutually opposite SMSWs propagation. The rejection pit frequency of the device is shifted by the frequency of the SAW at the inversion of the direction of propagation of SMSW in accordance with the Eq. (1). The frequencies of the rejection pits are determined by the frequency of SAW. It was possible to adjust the stop-band frequencies in a certain limit by changing the frequency of the SAW, herewith the frequency shift between the frequencies of the rejection pits at the inversion of the direction of propagation of the SMSW also changed. The measured dependencies of the frequencies of the rejection pits, f_R , as a function of SAW frequency, F , for two mutually opposite directions of SMSW propagation are given in Fig. 4.

SAW in this experiment was excited by the IDT nearest to the port 1. In our experiment, these dependencies are practically linear at a given YIG film thickness and relatively narrow range of SAW frequency change. Solid lines in Fig. 4 were calculated using [25] without taking into the account the influence of magnetic anisotropy and waves attenuation at propagation and provided that the dispersion characteristics of SMSW in structure are the same for both directions of propagation. As follows from the results presented in Fig. 4 in our model, changing the frequency of the SAW, ΔF , by 1 MHz leads to a shift in the notch frequency, Δf_R , by ~ 7 MHz. In general, $\Delta f_R = k\Delta F$ is described by the steepness of the governing characteristic $k = \left. \frac{\partial f_R}{\partial F} \right|_F$, determined by the shape of the dispersion characteristic of SMSW, by the frequency of SAW and in certain conditions can reach 10 or more. Expression (2) permits to calculate k as functions of H_0 – external magnetic field, d – the thickness of YIG film and F :

$$k = \frac{f_m^2 \pi d}{4 v_{SAW}} \exp\left(-\frac{2\pi F d}{v_{SAW}}\right) \cdot \frac{1}{f_R} \quad (2)$$

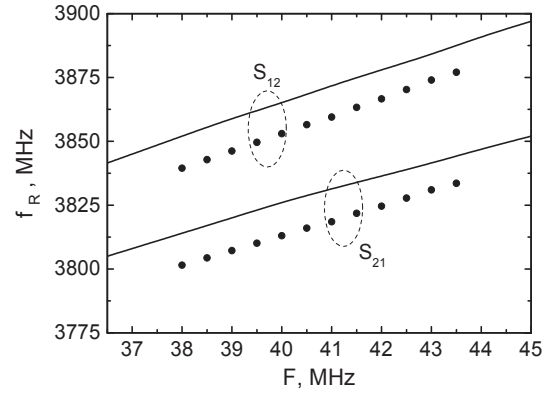


Fig. 4. The frequency of rejection, f_R , as a function of the SAW frequency, F . Experimental points - measured from the AFC of the parameter S_{12} (SMSW and SAW propagate in the same direction) and from the AFC of the parameter S_{21} (SMSW and SAW propagate in opposite directions). The solid lines are the calculations. The sample parameters are given in the caption to Fig. 3. SAW velocity in the structure is taken equal to $3.33 \cdot 10^5$ cm/s [20].

Here: $f_R = \left[f_O^2 + \frac{f_m^2}{4} (1 - e^{-\frac{2\pi F d}{v_{SAW}}}) \right]^{1/2}$, $f_m = \gamma 4\pi M_0$; $f_O^2 = f_H^2 + f_H f_m$; $f_H = \gamma H_0$; γ – gyromagnetic ratio, M_0 – the saturation magnetization of YIG; d – the thickness of YIG film.

The expression (2) was obtained by solving together Eqs. (1) and Damon-Eshbach dispersion equation for SMSW [28], without taking into the account the influence of magnetic anisotropy and waves attenuation at propagation, provided that the dispersion characteristics of SMSW in structure are the same for both directions of propagation and $F \ll f_R$. Δf_R calculated from (2) at $\Delta F = 1$ MHz with our experimental parameters was indeed 7 MHz. With decreasing of F , Δf_R increases, as the interaction of SAW and SMSW occurs at a steeper section of the dispersion curve (see Fig. 1), where the group velocity of SMSW is greater, at $F = 20$ MHz $\Delta f_R = 9$ MHz, at $F = 10$ MHz $\Delta f_R = 12$ MHz. At $H = 400$ Oe and at $F = 10$ MHz (2) gives $\Delta f_R = 15$ MHz.

The width of the notch (rejection) pit is determined by the width of the magnonic stop-band of SAW-MC and at the conditions of our experiment is depends only on SMSW attenuation value [20,21]. The notch depth is controlled by the power of the SAW. The notch depth as a function of SAW power for the sample under investigation is presented in Fig. 5. Thus, the notch frequency and the rejection depth in the SAW-MC notch filter can be adjusted within certain limits, changing the frequency and power of the SAW. As noted in the Introduction, spin-

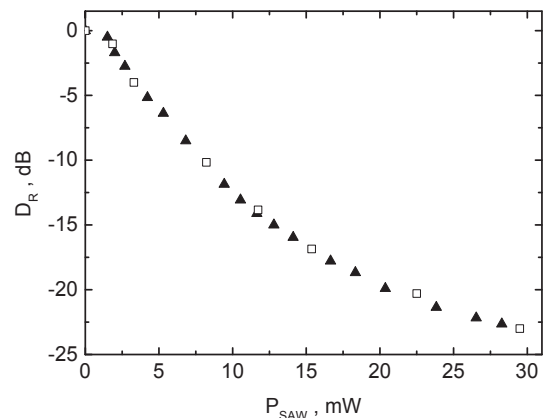


Fig. 5. Measured notch depths, D_R , as a function of the power of the SAW, P_{SAW} , in the magnonic crystal. Experimental points in the form of triangles-measurements at $f_R = 3818$ MHz at the counter-propagation of SMSW and SAW, hollow squares at the frequency $f_R = 3859$ MHz at the co-propagation of SMSW and SAW. Other experimental conditions as in Fig. 3.

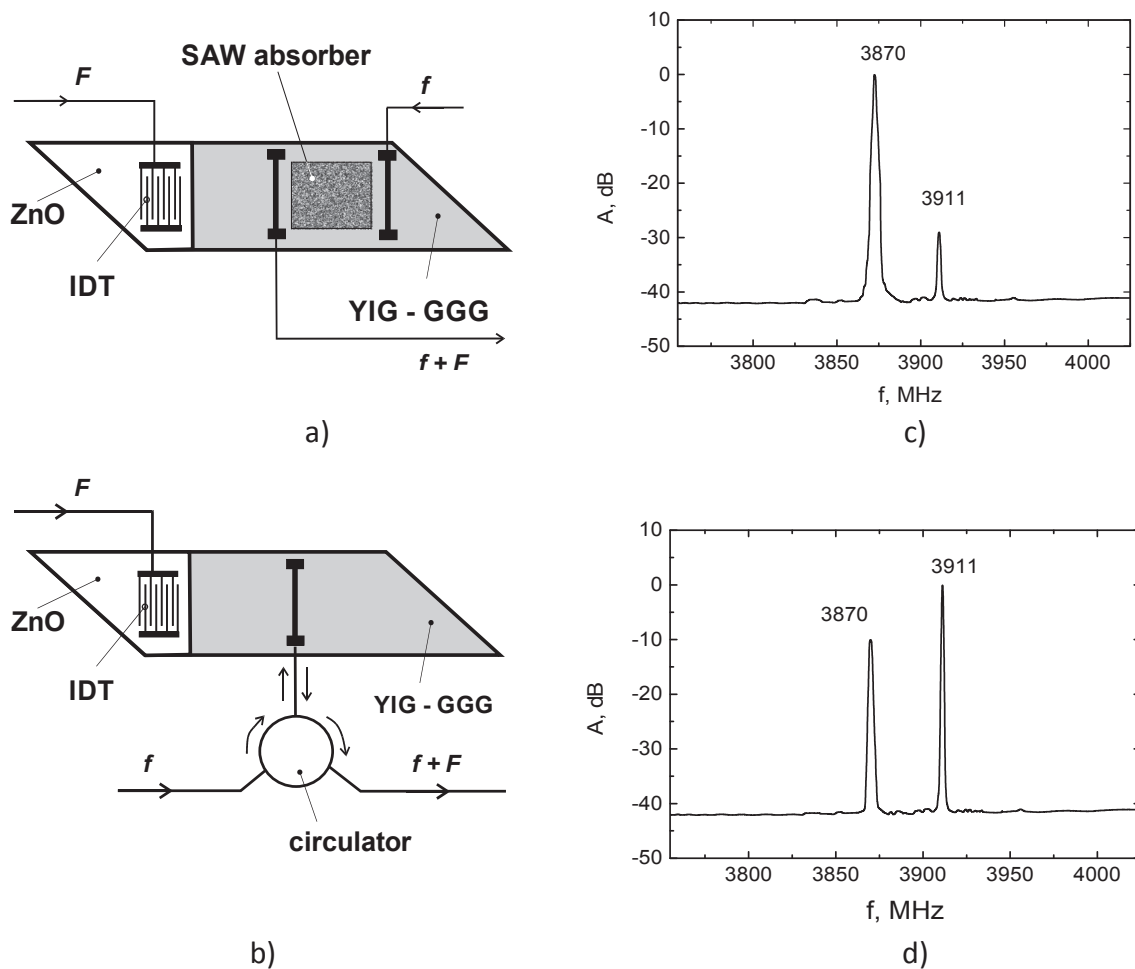


Fig. 6. Two designs of the frequency shifting device (top view) on the base of the SAW-MC and their measured output spectra. YIG film 8,4 μm , ZnO film 5, 5 μm . IDT: 14 pairs of aluminum electrodes with 80- μm -period. Apertures of IDT and antenna 5 mm. $H_0 = 640$ Oe. $T_0 = 20^\circ\text{C}$. SAW frequency $F = 41$ MHz, SAW power $P_{\text{SAW}} = 5\text{mW}$. (a) with two antennas, (b) with one antenna and circulator, (c) its output spectrum, (d) its output spectrum.

wave devices usually have insufficient temperature stability of the parameters and the possibility of such adjustment will help to overcome this drawback.

Frequency tuning of the device, as other spin wave devices, can also be carried out by changing the biasing magnetic field [6].

4. Frequency shifting and modulating

Another example of application of SAW-MC for microwave signal processing may serve suggested devices for frequency shifting and frequency modulation. Two possible designs of these devices are presented in Fig. 6. In both designs the basis is the SAW-MS using monolithic structures GGG - YIG film - ZnO film, as in the case of notch filters described in previous section. The first design has two antennas (see Fig. 6a): one antenna for exciting the SMSWs and the other is used for signal's output. To excite the SAW, as in the layout of the notch filter, used an IDT, deposited on the surface of the ZnO film. The main parameters of this IDT are given in the caption to Fig. 6. The principle of operation of the devices explains Fig. 1. When the SMSW of corresponding frequency f and SAW of frequency F are excited and propagate in the sample, the signals of frequencies f and $f + F$ appear at the output antenna in accordance with the Eq. (1) (see also Fig. 1). Setting the required operating frequency of the device is made by changing the external magnetic field as in any other devices based on the magneto-static waves.

At a fixed magnetic field, the signal with the shifted frequency will

appear only in a rather narrow frequency band of the input signal defined by the external magnetic field and YIG film parameters.

The second design has a single antenna common for the excitation of SMSW and for the reception of the shifted output signals of $f + F$ frequencies. This single antenna is connected to external circuits through the circulator (Fig. 6b). This design can significantly reduce the level of the frequency f at the output of the device compared to the design with two antennas. The output spectra for two designs are given in Fig. 6c and d. It is seen, the level of the signal with the frequency f is rather high in both constructions in our experiment. However, in the design of a single antenna with a moderate SAW power of less than 3 mW, the signal level with frequency f can be significantly reduced, by 20 dB or more, when using a circulator with interchannel isolation of more than 20 dB. In this case, the impedances of the antenna and external circuits must be matched well. The dynamic range of these devices is the same as that of all linear SNSW devices [6,23]. These devices can be used for frequency modulation as well, with the output spectrum having only one side frequency (no mirror frequency).

5. Conclusion

The concept of dynamic magnonic crystals with SMSW was shown to be useful for creating unique nonreciprocal notch filters tuning by SAW and for other microwave devices. Examples of SAW-MC based prototypes of devices, described in this paper, illustrate the principal mechanisms of their operation and application possibilities of SAW-

MCs. The experimental parameters of devices obtained in the present work can by no means be considered as ultimate since the objective of the work was to demonstrate operation ability of the prototypes of the devices based on SAW-MC. To improve of parameters of suggested devices the optimization of their designs must be done.

It should be noted, that not all known to date useful properties of SAW-MC, that could be used for the creation of signal processing devices, were involved in the development of prototypes of devices described in this work. As our estimations [22] show, the features of SAW-MC due to magnetic anisotropy of YIG films investigated in [22], when using for notch filters applications, would reduce the required power of SAW by an order of magnitude to achieve the same parameters as those obtained in this paper.

References

- [1] Morgan, David P. *Surface-wave Devices for Signal Processing*. North-Holland, 1991.
- [2] Clemens C.W. Ruppel, Tor A. Fjeldly, *Advances in Surface Acoustic Wave Technology, Systems and Applications*, World scientific, 2001.
- [3] Y.V. Gulyaev, F.S. Hickernell, *Acoustoelectronics: history, present state, and new ideas for a new era*, *Acoust. Phys.* 51 (1) (2005) 81–88.
- [4] C. Campbell, *Surface Acoustic Wave Devices and Their Signal Processing Applications*, Elsevier, 2012.
- [5] F.R. Morgenthaler, *Micro. J.* 25 (1982) 83–90.
- [6] Waguih S Ishak, *Proc. IEEE* 76.2 (1988) 171–187.
- [7] A.A. Serga, A.V. Chumak, B. Hillebrands, *J. Phys. D: Appl. Phys.* 43 (26) (2010) 264002.
- [8] A. Khitun, M. Bao, K.L. Wang, *J. Phys. D: Appl. Phys.* 43 (26) (2010) 264005.
- [9] A.V. Chumak, A.A. Serga, B. Hillebrands, *Nat. Commun.* 5 (2014) 4700.
- [10] A. Acevedo, I. Gomez-Arista, O. Kolokoltsev, M.M. Sánchez, R.C. Guzmán, *Electron. Lett.* 54 (7) (2018) 418–420.
- [11] A.V. Chumak, V.I. Vasyuchka, A.A. Serga, B. Hillebrands, *Nat. Phys.* 11 (6) (2015) 453–461.
- [12] A.V. Chumak, A.A. Serga, B. Hillebrands, *J. Phys. D: Appl. Phys.* 50 (24) (2017) 244001.
- [13] M. Krawczyk, D. Grundler, *J. Phys.: Condensed Matter* 26 (12) (2014) 123202.
- [14] H. Puzkarski, M. Krawczyk, *Phys. Lett. A* 282 (1) (2001) 106.
- [15] Yu.V. Gulyaev, S.A. Nikitov, L.V. Zivotovskii, A.A. Klimov, Ph. Tailhades, L. Presmanes, C. Bonningue, T.S. Tsai, S.L. Vysotskii, Y.A. Filimonov, *JETP Lett.* 77 (2003) 567.
- [16] R.A. Gallardo, T. Schneider, A. Roldán-Molina, M. Langer, J. Fassbender, K. Lenz, P. Landeros, *Phys. Rev. B* 97 (14) (2018) 144405.
- [17] A.V. Sadovnikov, S.A. Odintsov, E.N. Beginin, A.A. Grachev, V.A. Gubanov, S.E. Sheshukova, S.A. Nikitov, *JETP Lett.* 107 (1) (2018) 25–29.
- [18] A.V. Chumak, T. Neumann, A.A. Serga, B. Hillebrands, M.P. Kostylev, *J. Phys. D: Appl. Phys.* 42 (20) (2009) 205005.
- [19] A.A. Nikitin, A.B. Ustinov, A.A. Semenov, A.V. Chumak, A.A. Serga, V.I. Vasyuchka, B. Hillebrands, *Appl. Phys. Lett.* 106 (10) (2015) 102405.
- [20] R.G. Kryshchal, A.V. Medved, *Appl. Phys. Lett.* 100 (19) (2012) 192410.
- [21] R.G. Kryshchal, A.V. Medved, *J. Magnet. Magn. Mater.* 395 (2015) 180–184.
- [22] R.G. Kryshchal, A.V. Medved, *J. Magnet. Magn. Mater.* 426 (2017) 666–669.
- [23] R.G. Kryshchal, A.V. Medved, *J. Phys. D: Appl. Phys.* 50 (49) (2017) 495004.
- [24] A.M. Mednikov, A.F. Popkov, V.I. Anisimkin, B.P. Nam, A.A. Petrov, A.A. Spivakov, A.S. Khe, *JTEP Lett.* 33 (1981) 646.
- [25] A.F. Popkov, *Fiz. Met. Metalloved* 59 (1985) 463.
- [26] S.M. Hanna, G.P. Murphy, K. Sabetfakhri, K. Stratakis, 1990 *IEEE Ultrason. Symp. Proc.*, 1990, p. 209.
- [27] R.G. Kryshchal, A.V. Medved, A.F. Popkov, *J. Commun. Technol. Electron.* 39 (1994) 132.
- [28] R.W. Damon, J.R. Eshbach, *J. Phys. Chem. Solids* 19 (1961) 308.